Fabrication of GaN-based nanoscale device structures utilizing focused ion beam induced Pt deposition

Abhishek Motayed[*]

Material Science and Engineering Laboratory, National Institute of Standards and Technology, Gaithersburg, Maryland 20899 and Department of Electrical and Computer Engineering, University of Maryland, College Park, Maryland 20742

Albert V. Davydov, Mark D. Vaudin, and Igor Levin

Material Science and Engineering Laboratory, National Institute of Standards and Technology, Gaithersburg, Maryland 20899

John Melngailis

Department of Electrical and Computer Engineering, University of Maryland, College Park, Maryland 20742

S. N. Mohammad

Department of Material Science and Engineering, University of Maryland, College Park, Maryland 20742 and Department of Electrical and Computer Engineering, Howard University, Washington, DC 20059

(Received: 13 December 2005; accepted: 16 May 2006; published online: 20 July 2006)

In this work we have demonstrated nanoscale GaN device structures made from individual GaN nanowires and electrical contacts utilizing focused ion beam (FIB) induced Pt deposition. These GaN nanowires were grown by direct reaction of Ga vapor with NH_3 and had diameters ranging from 100 nm to 250 nm and lengths up to 200 μm. As-grown nanowires were dispersed on SiO_2 coated p^{++} Si substrate. A 30 keV Ga^+ ion beam was used to dissociate (trimethyl)methylcyclopentadienyl-platinum precursor for depositing Pt contacts to GaN nanowires. FIB-deposited Pt contacts to GaN nanowires showed nonlinear *I-V* characteristics, which turned linear after annealing at 500 °C for 30 s in argon. Resistivity of a GaN nanowire measured using a four terminal contact geometry fabricated by depositing Pt with a FIB was in the range of 5×10^{-3} Ω cm. Temperature dependent resistivity measurement of the GaN nanowire revealed semiconducting behavior with a weak temperature dependence of the resistivity. In this study both Ohmic and Schottky contacts to GaN nanowires have been realized with FIB-

deposited Pt contacts. Barrier height and ideality factor have been extracted for the metal-GaN nanowire Schottky junctions, which had low reverse breakdown voltage and large ideality factor of 18. Modulation of the current through the nanowire was achieved by applying a bias to the Si substrate acting as a backgate. *n*-type depletion mode behavior was observed in the GaN nanotransistor, which was consistent with the impurity related background concentrations expected in this type of growth method. The heat generation during FIB deposition and the ion damage appeared to cause noticeable swelling of the nanowires under the Pt contacts. Electron beam induced Pt deposition was also used to fabricate electrical contacts to the nanowires. ©2006 *American Institute of Physics*

Contents

INTRODUCTION

Nanoscale semiconducting materials and structures are promising elements for realizing highly efficient electronic and optoelectronic devices and studying fundamental transport properties in mesoscopic systems.[1,2,3,4,5] The Group IIIA nitrides (binary and ternary alloys of AlN, GaN, and InN) have unique properties such as a band gap spanning the whole solar spectrum (from 0.7 eV for InN to 6.2 eV for AlN), high saturation velocity, and high breakdown electric field. As a result nanostructures and nanodevices made from GaN and related nitrides have great potential for realizing next generation efficient nanoscale UV/visible light emitters, detectors, and high temperature electronic devices. Although significant progress has been made in semiconducting nanowire growth,[6,7,8,9] further optimization of the growth processes is still required. Positioning them on a suitable substrate for device fabrication often involves complex aligning procedures such as electric field assisted aligning,[5] microfluidic aligning, and chemical patterning.[10] These procedures are time consuming and require elaborate substrate prepatterning. Perfecting these alignment techniques is necessary in order to realize hierarchical assembly for large scale nanosystem development. However, for growth optimization and study of transport properties of individual nanowires, versatile fabrication methods suitable for random nanowire orientations have to be developed.

We have demonstrated that, by utilizing focused ion beam (FIB) induced metal deposition techniques, we can fabricate prototype devices and extract material properties of individual GaN nanowires, such as resistivity and electron mobility of individual GaN

nanowires without elaborate alignment and fabrication techniques. GaN nanowires for this study were grown by direct reaction of Ga vapor with NH_3 at 900 °C. Comprehensive structural characterizations with transmission electron microscopy (TEM), x-ray diffraction (XRD), and electron backscattered diffraction (EBSD) were performed to determine the crystalline quality and orientation of the nanowires. Present study focuses on the viability of FIB metal deposition technique for rapid prototype device structure fabrication using GaN nanowires.

EXPERIMENTAL PROCEDURE

The GaN nanowires used for this study were grown by direct reaction of metal gallium vapor with flowing ammonia at 850 °C–900 °C in a horizontal furnace, as described elsewhere.[6] Figure 1 schematically shows the experimental setup for nanowire synthesis, where Ga metal (~99.999% pure) was put in a small boron nitride boat and placed at the bottom of a quartz liner. Ammonia (~99.999% pure) was introduced at a rate of 50 SCCM–100 SCCM (SCCM denotes cubic center per minute at STP), with the growth temperature set between 850 °C and 900 °C for 3 h–4 h. Depending on the growth temperature and reactor pressure, lengths and diameters of these nanowires can be varied.[9] The growth results in a matrix on the boron nitride boat and quartz liner, containing single crystal GaN nanowires together with GaN platelets.

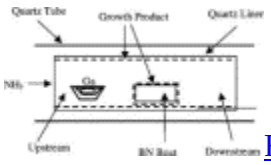

Figure 1.

After completion of the growth, the GaN matrix with nanowires was collected from the inner lining of the furnace, and then sonicated in isopropanol to achieve a dilute suspension of nanowires. The suspension was then dispersed on SiO_2 (150 nm thick) coated Si substrate (p^{++}, ρ=0.5 Ω cm) with predefined Cr/Au pads. Locations of the nanowires with respect to the pads were noted with an optical microscope. A dual beam FEI 620 FIB/SEM (Ref. 11) tool was used with (trimethyl)methylcyclopentadienyl-platinum (STREM Chemicals 99%) as an organometallic precursor to deposit Pt contacts to these nanowires. A 30 keV Ga^+ ion beam was used with 7 pA current aperture during ion beam deposition. It was observed that using higher current apertures causes significant sputtering of the nanowires before metals start depositing. Dwell time and overlap for the Ga^+ ion beam were 0.4 μs and 0%, respectively. Using these deposition parameters, Pt contacts with nominal dimensions of 2 μm in width, 20 μm in length, and approximately 1 μm in height were routinely deposited.

In order to achieve linear *I-V* characteristics the FIB-deposited Pt contacts were annealed at 500 °C for 30 s in ultrahigh purity (UHP)-grade argon using a rapid thermal annealing furnace. *I-V* characteristics of the GaN nanowire were measured using an HP4140B picoammeter. A Keithley 238 source measure unit was used to measure the four terminal resistivity of the nanowire. Schottky diode to GaN nanowire was realized by using as-deposited Pt contact. The Ohmic contact for the diode was formed by annealing another

Pt contact, which was FIB-deposited prior to the Schottky contact. The barrier height and ideality factor for the diode were extracted from the *I-V* characteristics. Metal-oxide semiconductor field-effect transistor (MOSFET) type of transistor action was obtained from individual GaN nanowire with source and drain contacts formed by annealed FIB Pt contacts and Si substrate as the global backgate. A Hitachi S4700 field emission scanning electron microscope (FESEM) was used to study the morphology of the metal-nanowire contact region. EBSD was carried out using the same FESEM at voltages of 15 and 20 keV using an emission current of 20 nA. Careful background subtraction was necessary as the electron beam frequently was able to penetrate through the nanowires and diffract from the underlying substrate. Simulation of 30 keV Ga^+ ions impinging on GaN nanowires was carried out using SRIM 2003 (Ref. 12) software to study the interaction of Ga^+ ions with the nanowire. Electron beam induced deposition of Pt on nanowires was carried out using the same dual beam FEI system to investigate the effect of heating in the nanowires under the charged particle beams.

RESULTS AND DISCUSSIONS

GaN matrix with attached nanowires as collected from the growth chamber is shown in the FESEM image in Fig. 2(a). This matrix consists primarily of two distinct features, viz., single-crystalline GaN nanowires and GaN platelets. The diameters of these platelets range from 0.5 μm up to 5 μm, and it has been confirmed by EBSD that the normal of these GaN platelets is the *c* axis of the wurtzite structure. From Fig. 2(b) it appears that the nanowires grow from the side facets of GaN platelets, which corresponds to *a* planes of the wurtzite structure. Thus the nanowire axis was also in the *a* direction as confirmed by EBSD (see Fig. 3). EBSD also showed that some nanowires were split into bicrystals with the *a* axes of both crystals aligned with the wire axis. Thus the misorientation axis for the bicrystal was also the *a* axis; the misorienatation angles varied from 45° to 85°. Electron diffraction in TEM confirmed the nanowire axis to be parallel to the [10–10] direction, consistent with the EBSD results. Many nanowires represented a bundle of several crystals (Fig. 4) featuring similar growth direction and grown together so that the intercrystal boundaries were parallel to the wire axis. The complex crystallography exhibited by these multiple crystal assemblages within the individual nanowires is a subject of a continuing investigation.

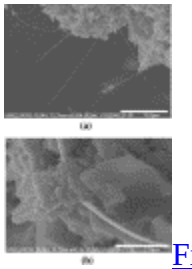

Figure 2.

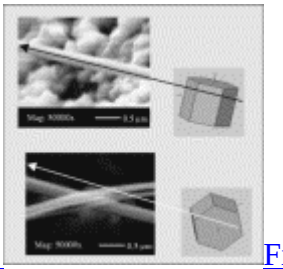

Figure 3.

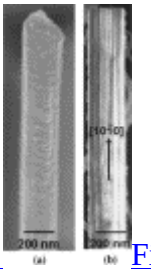

Figure 4.

After sonication and dispersion of the nanowires on the prepatterned substrates, the nanowires were found to have a tendency to lie on or close to the metal pads, as shown in Fig. 5. We can speculate that this was due to the difference in the evaporation rates of the solvent over the pad and the SiO_2 substrate, which causes the wires to deposit close to the

pads. Alternatively the surface charges of the nanowires can give rise to image charges inside the metal, hence creating an electrostatic force of attraction between the metal and the nanowire. After the nanowire lands on the pad and the solvent dries out, van der Waals forces might hold the nanowires to the susbstrate.

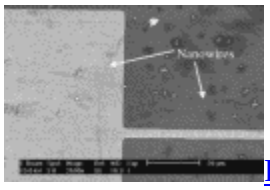

Figure 5.

After dispersion of the nanowires, the FIB was used to deposit Pt pads to contact these nanowires. Figure 6 shows a single nanowire contacted at the ends using two FIB-deposited Pt lines. Current-voltage characteristics of the nanowire measured using the as-deposited Pt contacts were nonlinear, with current level in range of 1.5×10^{-9} A for 10 V bias, as shown in Fig. 7(a). This is expected, as it has been observed that Pt, with work function of 5.65 eV, when deposited on *n*-GaN generally forms Schottky contacts.[13] Although it is suitable to have a low work function metal such as Ti or Al for making low resistance Ohmic contacts to *n*-GaN,[14] it has been demonstrated that annealing metals such as Ni, with a work function of 5.15 eV, can make Ohmic contacts with fairly low specific contact resistance.[15] Similarly, in our case, annealing the contacts in UHP argon at 500 °C for 30 s resulted in linear contact behavior, as seen in Fig. 7(b). Notably, the current level increased four orders of magnitude after the anneal. We speculate that the annealing of the Pt contacts formed Ga–Pt intermetallics. Indeed, formation of intermetallic phases such as Ga_3Pt_5 has been observed when Pt on GaN was annealed at 600 °C.[16] Formation of Pt gallides may lead to lowering of the contact barrier height due to the lower work function of the Ga–Pt intermetallics, which should lower contact resistance. Also, when Pt reacts with GaN, it will create defects in the crystal structure underneath the contact area, thus enhancing the conductivity via tunneling through the defects. It might be possible that both factors contributed to the lowering of the contact resistance. From the *I-V* characteristics of the nanowire with annealed contacts shown in Fig 7(b), the calculated two terminal resistance was 50 kΩ. The current densities recorded in the nanowires are in the region of 5.0×10^{5} A cm^{-2} for bias voltage of 3 V which is significantly higher than what has been reported so far.[17,18] Higher current densities are beneficial for realizing efficient light emitting devices. Contact characteristics were very stable, with no Joule heating observed in the contacts with prolonged current flow.

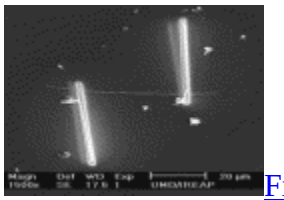
Figure 6.

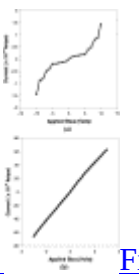
Figure 7.

Figure 8 is an optical microscope image of a GaN nanowire with FIB-deposited four terminal Pt contact structure, which was used to measure the resistivity of the nanowire. Current was forced through the end contacts, and subsequently the voltage drop was measured using two inner electrodes (termed as voltage probes). The resistivity of the GaN nanowire measured using the four terminal configurations was in the range of 5×10^{-3} Ω cm. Although these nanowires are not intentionally doped, the lower value of the resistivity observed in these nanowires compared to bulk GaN could be due to the nitrogen vacancies or residual contaminants such as oxygen, which contribute to the background carrier concentration. High background carrier concentrations has been often noticed in these types of growth chambers.[19] In order to understand the effect of the resistance of FIB Pt contacts on the resistivity measurements of the nanowires, we measured the resistivity of FIB-deposited Pt contacts utilizing a four terminal configuration. It is well accepted that the resistivity of the FIB-deposited Pt is around 5.0×10^{-4} Ω cm,[20] which is generally an order higher than the value of bulk Pt (1.06×10^{-5} Ω cm). Using similar deposition parameters as used to make contacts to the nanowires, we deposited a Pt line 2 μm wide, 60 μm long, and 1 μm thick onto a prepatterned four terminal Cr/Au structure, as shown in Fig. 9. The resistivity of FIB-Pt obtained was 9.0×10^{-4} Ω cm, which is a little higher than the accepted value. The resistivities of FIB-deposited metals are known to have a sensitive dependence on the deposition parameter.[21]

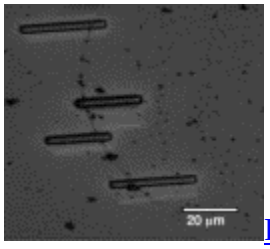

Figure 8.

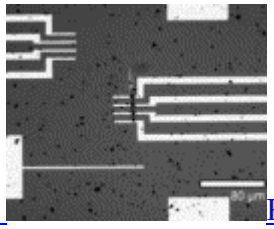
Figure 9.

Figure 10(a) is a schematic diagram of the four terminal structure used for resistivity measurement of nanowire. Although similar type of structure has already been used to measure the resistivity of both the metallic[22] and semiconducting nanowires,[23,24] the effect of the voltage probes in the resistivity measurement of these nanowires has not been investigated. For metallic nanowires voltage probes will not have any significant effect on the resistivity measurements. Generally the metals deposited to make contacts to the nanowire using electron beam deposition, FIB, or any other technique will always cover the entire periphery of the nanowire. This induces depletion effect over the entire cross sectional area of the nanowire, which will extend laterally beyond the contact periphery, as shown in Fig. 10(b). This will reduce the effective length of the nanowire used for calculating the resistivity, thus leading to underestimation of the resistivity. One possible way to minimize this error is to cover the nanowire in a dielectric layer (i.e., SiO_2, Si_3N_4) and to use vias to make contact between the voltage probes and the top part of the nanowire. In this way the depletion width associated with the probe will be limited to only the top portion of the nanowire, thereby reducing the error in resistivity measurement.

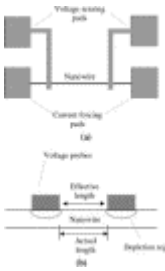

Figure 10.

In order to understand the nature of the transport through the nanowires we conducted temperature dependent resistivity measurement of the nanowire. Figure 11(a) is the plot of the resistivity of a GaN nanowire as a function of the temperature from 30 °C to 100 °C. Semiconducting behavior is clearly seen from the nanowire, the resistivity decreasing with increasing temperature, with a weak temperature dependence of the resistivity. For metallic nanowires, the resistivity should have increased with the temperature. Although it is evident from the activation energy plot in Fig. 11(b) that the transport cannot be simply described using the simple thermal activation energy resistivity model as given by

$$\ln \rho = \ln \rho_0 + \left(\frac{E_a}{k}\right) T^{-1}, \qquad (1)$$

where ρ is the resistivity of the nanowire, ρ_0 is a characteristic constant, and E_a is the activation energy, yet some important features of the transport through the nanowire can be qualitatively pointed out from these results. Two distinct slopes representing two different activation energies can be clearly seen in Fig. 11(b). In the range of 30 °C–60 °C, the activation energy E_a is 20.0 meV, and for the range of 60 °C–100 °C the E_a is 2.4 meV. At higher temperatures (above 60 °C) the thermal generation of excess charge carrier across the band gap may lead to a stronger electron-electron and electron-phonon interactions thus leading to less variation in the resistivity of nanowire with temperature. The weak temperature dependence of the resistivity of the nanowire may be a signature of the electron-electron interactions in a two-dimensional disordered system, since the nanowires used for this study has structural defects and impurities. In order to gain a better understanding of the transport properties of these nanowires, the resistivity measurements has to be performed at lower temperatures (liquid He of 4.2 K).

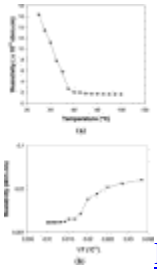

Figure 11.

We have fabricated FIB-deposited Pt Schottky contacts to these GaN nanowires, with prefabricated Ohmic contact formed by annealing FIB Pt contacts at 500 °C for 30 s in

UHP argon. Measured *I-V* characteristics of the Pt–GaN nanowire junction from which we derived the ideality factor and the barrier height are presented in Fig. 12(a). Figure 12(b) is a semilog plot of the measured *I-V* curved of the Pt–GaN nanowire diode. From the *I-V* characteristics it is evident that the FIB-deposited Pt–GaN nanowire diode suffers from large reverse bias leakage current with reverse breakdown voltage around 4 V. This diode had low forward turn-on voltage (0.8 V) and soft reverse breakdown characteristics, which indicated that the tunneling mechanism might be the dominant mode of conduction in this diode. Current density *J* through a Schottky barrier junction resulting from the conventional thermionic emission can be expressed as

$$J = J_0 \left[\exp\left(\frac{qV}{\eta kT} \right) - 1 \right], \qquad (2)$$

where J_0 is the reverse saturation current density given by

$$J_0 = AT^2 \exp\left(\frac{q\phi_b}{kT} \right), \qquad (3)$$

where *A* is the Richardson constant (assumed to be 26 A cm^{-2} K^{-2} for GaN),[25] *V* is the applied voltage, *q* is the electronic charge, *T* is the absolute temperature of the metal-semiconductor junction, ϕ_b is the Schottky barrier height of the metal-semiconductor junction, and η is the ideality factor which represents the extent of nonideality of the metal-semiconductor junction. Using Eqs. (2),(3) and the plot in Fig. 12(b), the ideality factor η and the barrier height ϕ_b were calculated to be 18 and 0.2 eV, respectively, which is reminiscent of the fact that these diodes are nonideal probably due to the ion damage occurring during FIB deposition at the surface of these nanowires. The detrimental effects of the ion damage on the electrical properties (increase in leakage current and reduction in reverse breakdown voltage) of Schottky diodes fabricated on epitaxial nitrides has been already demonstrated.[26] Thus we believe that the ion damage and the excess Ga^+ implantation during Pt deposition resulted in higher leakage current and lower barrier height of these diodes.

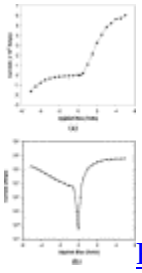

Figure 12.

MOSFET-type transistor action from these nanowires has been achieved by depositing Al metal on the backside of the Si substrate as the backgate. Annealed FIB-deposited Pt contacts served as the source and drain contacts. Figure 13 is the plot of the source-drain

current (I_{DS}) versus source-drain voltage (V_{DS}) as a function of different gate voltages for a single GaN nanowire. It can be clearly seen that the device exhibits an *n*-type depletion mode behavior, which is due to the unintentional *n*-type background concentration. Transconductance was calculated to be around 10 ms/mm with mobility of 20 $cm^2\ V^{-1}\ s^{-1}$. The mobility is low compared to the bulk mobility of GaN, which is expected due to the disordered nature of these nanowires.

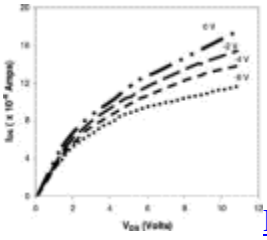

Figure 13.

Careful investigation of the FIB Pt–GaN nanowire contact areas under SEM revealed an interesting feature. From Figs. 14(a)14(b), noticeable swelling of the nanowire underneath the FIB-deposited Pt contact can be clearly seen. Although similar nanowire swelling underneath the FIB-deposited contacts was observed in other experiments,[27,28] the reasons for this effect has not yet been discussed. The study on Ga^+ self-implanted GaN nanowires[29] has revealed the formation of "nanoblisters" and volume expansion of the nanowires after Ga^+ ion irradiation of the nanowires. Volume swelling and lattice damage of the GaN nanowires observed in the study was correlated to the large scale disintegration of Ga from the lattice and partially accumulation inside the nanoblisters. In order to gain a better understanding of the interactions of Ga^+ ion with GaN nanowires, we conducted simulation of the ion implantation of Ga^+ ions into the nanowires using Monte Carlo based STRIM code. Simulations showed that for implantation of 30 keV Ga^+ ions into GaN, the nuclear energy loss mechanism is the dominant one with nuclear stopping power about 1.96 keV nm^{-1} which was an order of magnitude higher than the electron stopping power. The projected range for 30 keV Ga^+ was about 15 nm, which indicates that most of kinetic energy of these ions is transferred to the GaN nanowire lattice. This could lead to a significant rise in temperature of the nanowire. The heat generation in the nanowire during the FIB induced Pt deposition could also contribute to the structural deformation observed in the nanowires. A simplified quantitative calculation has been performed to calculate the temperature rise of the nanowire during Pt deposition, using the amount of charge needed to deposit the small area of the contact immediately over the nanowire. Assuming very fast scan rate and negligible loss of energy of the Ga^+ ions during decomposition of the precursor, we calculated the total charge needed to deposit the small section of Pt line immediately over the nanowire (0.2 μm^2). The energy associated with that amount of charge was 1.485×10^{-6} J, which according to the calculations could lead to a temperature rise of about 400 °C in the nanowire. Although this temperature rise is not significant, it could lead to the partial decomposition and melting of GaN nanowire.

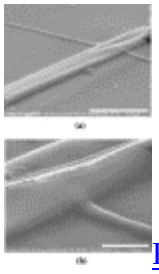

Figure 14.

In order to reveal the true nature of the effect of volume swelling of the nanowires, we conducted a parallel experiment and deposited Pt contacts to nanowires by electron beam induced deposition. Figure 15 shows the electron beam induced deposited Pt contacts ($0.8\times0.8\ \mu m^2$) to the nanowire. The electron beam energy was 10 keV, with 200 μA current aperture during the deposition. Close inspection revealed that there occurred a very similar swelling of the nanowire underneath Pt contacts deposited by electron beam. Although, small volume swelling is reported in electron-irradiated SiC due to the displacement of C and agglomeration of Si in the interstitial or antisite defect sites,[30] but the energy used in that study was 1 MeV. It is unlikely that the electrons with 10 keV energy are capable of causing that type of lattice damage. It is most likely that the heat generated by the focused Ga^+ beam during deposition was the main cause of the swelling of the nanowires underneath the contact area. Further studies are to be performed to determine the nature of the interaction of ions with these nanowires.

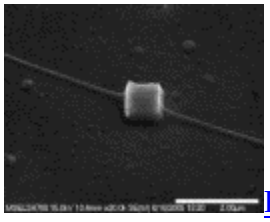

Figure 15.

CONCLUSION

In this work we have utilized focused Ga^+ ion beam induced metal deposition technique to deposit Pt contacts to GaN nanowires. As-deposited Pt contacts acted as Schottky contacts on the nanowires, while postdeposition 500 °C/30 s annealing converted them into Ohmic contacts. Basic device structures such as two-terminal resistor, Schottky diode, and MOSFET were realized on individual GaN nanowire using the FIB-deposited Pt contacts, without the need of prepatterning or aligning of the nanowires. Material properties such as resistivity and mobility have been obtained using these test structures. Significant interaction of Ga^+ ion beam and nanowire has been observed in a form of nanowire swelling under the Pt contact. Electron beam induced deposition of Pt on GaN nanowire revealed very similar swelling effect of the nanowire, which indicated that the likely cause of swelling of the nanowires is the heat generation during the focused Ga^+ ion beam deposition.

ACKNOWLEDGMENTS

Authors wish to thank John D. Barry of University of Maryland (IREAP) for his assistance with the use of the FIB tool, Dr. Maoqi He of Howard University for providing the nanowire samples, and Dr. Babak Nikhobakt for his assistance with the electron beam lithography.

REFERENCES

1. Y. Huang, X. Duan, Y. Cui, L. J. Lauhon, K.-H. Kim, and C. M. Lieber, Science **294**, 1313 (2001). [MEDLINE] first citation in article
2. A. Bachtold, P. Hadley, T. Nakanishi, and C. Dekker, Science **294**, 1317 (2001). [MEDLINE] first citation in article
3. X. Duan, Y. Huang, Y. Cui, J. Wang, and C. M. Lieber, Nature (London) **409**, 66 (2001). [MEDLINE] first citation in article
4. X. Duan, Y. Huang, R. Agarwal, and C. M. Lieber, Nature (London) **421**, 241 (2003). [MEDLINE] first citation in article
5. D. R. Bowler, J. Phys.: Condens. Matter **16**, 721 (2004). [ISI] first citation in article
6. M. He et al., Appl. Phys. Lett. **77**, 3731 (2000). first citation in article
7. M. H. Huang, Y. Wu, H. Feick, N. Tran, E. Weber, and P. Yang, Adv. Mater. (Weinheim, Ger.) **13**, 113 (2001). first citation in article
8. J.-R. Kim, H. M. So, J. W. Park, J.-J. Kim, J. Kim, C. J. Lee, and S. C. Lyu, Appl. Phys. Lett. **80**, 3548 (2001). first citation in article
9. A. M. S. ElAhl et al., J. Appl. Phys. **94**, 7749 (2003). [ISI] first citation in article
10. Y. Huang, X. Duan, Q. Wei, and C. M. Lieber, Science **291**, 630 (2001). [MEDLINE] first citation in article
11. Certain commercial equipment, instruments, or material supplier are identified in this paper in order to specify the experimental procedure adequately. This does not imply endorsement by NIST. first citation in article
12. J. F. Ziegler and J. P. Biersack, computer code SRIM 2003; http://www.srim.org first citation in article
13. K. Suzue, S. N. Mohammad, Z. F. Fan, W. Kim, O. Aktas, A. E. Botchkarev, and H. Morkoç, J. Appl. Phys. **80**, 4467 (1996). [ISI] first citation in article
14. A. Motayed, R. Bathe, M. C. Wood, O. S. Diouf, R. D. Vispute, and S. N. Mohammad, J. Appl. Phys. **93**, 1087 (2003). [ISI] first citation in article
15. A. Motayed, A. V. Davydov, L. A. Bendersky, M. C. Wood, M. A. Derenge, D. F. Wang, K. A. Jones, and S. N. Mohammad, J. Appl. Phys. **92**, 5218 (2002). [ISI] first citation in article
16. J.-S. Jang, S.-J. Park, and T.-Y. Seong, Appl. Phys. Lett. **76**, 2898 (2000). [ISI] first citation in article
17. Y. Huang, X. Duan, Y. Cui, and C. M. Lieber, Nano Lett. **2**, 101 (2002). first citation in article

18. G. Cheng et al., Appl. Phys. Lett. **83**, 1578 (2003). first citation in article
19. J.-R. Kim, B.-K. Kim, I. J. Lee, J.-J. Kim, J. Kim, S. C. Lyu, and C. J. Lee, Phys. Rev. B **69**, 233303 (2004). first citation in article
20. *Focused Ion Beam Workstations User Guide* (Technical Publication Department, FEI Company, Hillsboro, 1994). first citation in article
21. J. Melngailis, Proc. SPIE **1465**, 36 (1991). first citation in article
22. J.-F. Lin, L. Rotkina, and J. P. Bird, *Proceedings of the Second Quantum Transport Nano-Hana International Workshop*, 2004, IPAP Conf. Series, Vol. 5, p. 17. first citation in article
23. J. Goldberg, D. J. Sirbuly, M. Law, and P. Yang, J. Phys. Chem. B **109**, 9 (2005). [ISI] [MEDLINE] first citation in article
24. S. E. Mohney, Y. Wang, M. A. Cabassi, K. K. Lew, S. Dey, J. M. Redwing, and T. S. Mayer, Solid-State Electron. **49**, 227 (2005). first citation in article
25. M. Khan, T. Detchprohm, P. Hacke, K. Hiramatsu, and N. Sawaki, J. Phys. D **28**, 1169 (1995). first citation in article
26. A. Motayed, A. Sharma, K. A. Jones, M. A. Derenge, A. A. Iliadis, and S. N. Mohammad, J. Appl. Phys. **96**, 3286 (2004). first citation in article
27. Y.-J. Ma, Z. Zhang, F. Zhou, L. Lu, A. Jin, and C. Gu, Nanotechnology **16**, 746 (2005). first citation in article
28. C. Y. Nam, J. Y. Kim, and J. E. Fischer, Appl. Phys. Lett. **86**, 193112 (2005). [ISI] first citation in article
29. S. Dhara et al., Appl. Phys. Lett. **86**, 203119 (2005). [ISI] first citation in article
30. N. Asaoka, S. Muto, and T. Tanabe, Diamond Relat. Mater. **10**, 1251 (2001). [Inspec] [ISI] first citation in article

FIGURES

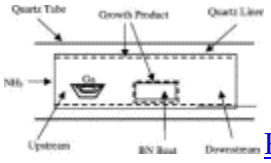

Full figure (8 kB)

Fig. 1. Schematic of the growth system used for the GaN nanowire growth. First citation in article

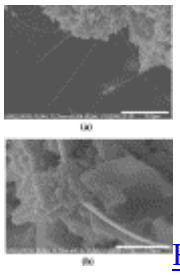
Full figure (21 kB)

Fig. 2. (a) FESEM scans of growth matrix after collecting from the growth chamber. (b) FESEM scans of nanowires growing from the edges of the GaN platelets. First citation in article

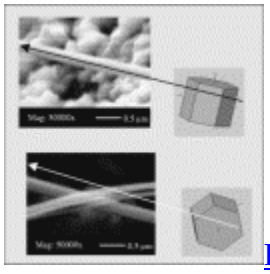
Full figure (19 kB)

Fig. 3. Electron beam backscattered diffraction showing that the growth direction of the nanowires is parallel to the *a* axis of GaN. The schematic crystal indicates the directions of the crystal axes. First citation in article

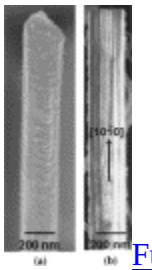

Full figure (17 kB)

Fig. 4. FESEM (a) and dark-field TEM (b) images of a typical GaN nanowire fragment. Many nanowires consist of multiple crystals sharing similar growth direction and having their interfaces aligned parallel to the nanowire axis. First citation in article

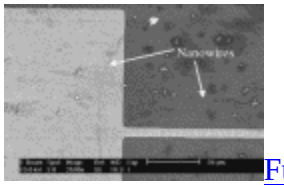

Full figure (14 kB)

Fig. 5. SEM image of nanowires dispersed on Cr/Au prepatterned pads on SiO_2 coated Si substrates. First citation in article

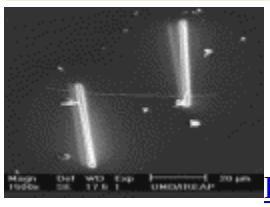
Full figure (9 kB)

Fig. 6. SEM image of a GaN nanowire with FIB-deposited Pt metal contacts at the two ends. First citation in article

---

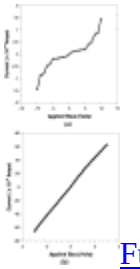
Full figure (20 kB)

Fig. 7. (a) Measured *I-V* characteristics of GaN nanowire with as-deposited FIB-deposited Pt contacts. (b) Measured *I-V* characteristics of the same nanowire after annealing the Pt contacts at 500 °C for 30 s in UHP argon. First citation in article

---

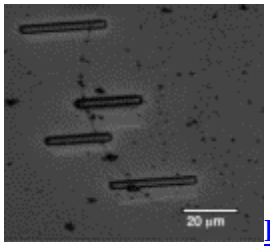

Full figure (6 kB)

Fig. 8. Optical microscope image of a GaN nanowire with FIB-deposited four terminal Pt resistivity measuring structure. First citation in article

---

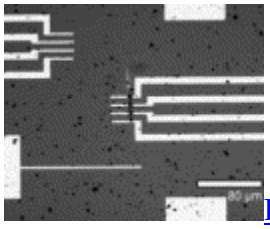
Full figure (10 kB)

Fig. 9. Optical microscope image of a FIB-deposited Pt line on a Cr/Au prepatterned four terminal structure. First citation in article

---

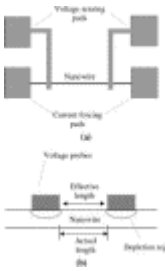
Full figure (12 kB)

Fig. 10. (a) Schematic diagram of the four terminal structure used to measure the resistivity of the nanowires. (b) Schematic of the nanowire with the voltage probes, the depletion region associated with the voltage probes shown by the dash line. First citation in article

---

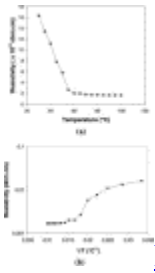
Full figure (9 kB)

Fig. 11. (a) Plot of resistivity (ρ) vs temperature of a GaN nanowire. (b) Activation energy plot of resistivity as a function of inverse temperature. First citation in article

---

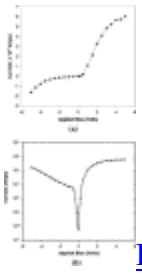
Full figure (11 kB)

Fig. 12. (a) *I-V* characteristics of FIB-deposited Pt–GaN Schottky diode (b) semilog plot of *I* vs *V* of the diode. First citation in article

---

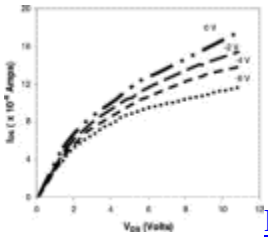
Full figure (7 kB)

Fig. 13. I_{DS} vs V_{DS} as a function of the gate voltage (V_G) applied to the Si backgate. The number on the each curve represents the gate voltage. First citation in article

---

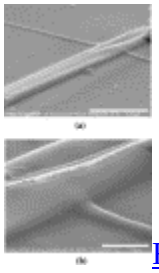

Full figure (13 kB)

Fig. 14. (a) SEM image of a FIB-deposited Pt line on GaN showing the volume swelling underneath the contact region. (b) High resolution SEM scan showing the swelling of the nanowire underneath the contact region. First citation in article

---

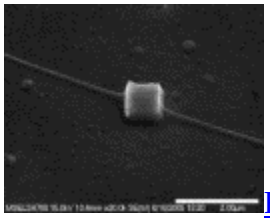

Full figure (6 kB)

Fig. 15. Electron beam induced deposited Pt contact to GaN nanowire. Swelling of the nanowire at the ends of the contacts are clearly visible. First citation in article

FOOTNOTES

*Author to whom correspondence should be addressed; electronic mail: amotayed@nist.gov

---